Calcium Protects Differentiating Neuroblastoma Cells during 50 Hz Electromagnetic Radiation

R. Tonini,* M. D. Baroni,* E. Masala,* M. Micheletti,† A. Ferroni,* and M. Mazzanti‡

*Dipartimento di Fisiologia e Biochimica Generali, I[a] Università di Milano, I-20133 Milano; †DIBIT, HSR, I-20100 Milano; and ‡Dipartimento di Biologia Cellulare e dello Sviluppo, Università "La Sapienza," I-00185 Roma, Italy

ABSTRACT Despite growing concern about electromagnetic radiation, the interaction between 50- to 60-Hz fields and biological structures remains obscure. Epidemiological studies have failed to prove a significantly correlation between exposure to radiation fields and particular pathologies. We demonstrate that a 50- to 60-Hz magnetic field interacts with cell differentiation through two opposing mechanisms: it antagonizes the shift in cell membrane surface charges that occur during the early phases of differentiation and it modulates hyperpolarizing K channels by increasing intracellular Ca. The simultaneous onset of both mechanisms prevents alterations in cell differentiation. We propose that cells are normally protected against electromagnetic insult. Pathologies may arise, however, if intracellular Ca regulation or K channel activation malfunctions.

INTRODUCTION

There is growing concern about the increase in environmental pollution due to the emission of electromagnetic waves. The mechanism of interaction between extremely low frequency electromagnetic fields (ELF-EMF) and biological structures, if it exists, is still obscure. Epidemiological studies have failed to find a correlation in live subjects between the continuous presence of ELF-EMFs at different intensities and the appearance of any particular pathology (Reipert et al., 1997; Lacy-Hulbert et al., 1998; Hatch et al., 1998; Day, 1999). However, several epidemiological studies have demonstrated increases in childhood leukemia and other related diseases in children from populations exposed to extremely low (50–60 Hz) frequency electromagnetic fields (Thomson et al., 1988) such as those produced by major power lines in the proximity of residential areas. However, none of these studies has found a significant correlation between the presence of ELF-EMFs and increases in pathological conditions. Likewise, not only do macroscopic analyses of cell survival using homogeneous primary cultures obtained from humans and animals show conflicting results, but investigations at subcellular level have also failed to explain the sporadic alterations observed after treatment with an ELF-EMF source (Reipert et al., 1997; Feychting et al., 1998). In general, if a detectable modification does exist, it is not constant and always occurs after activation of a complex cell mechanism (Hojevik et al., 1995; Grynkiewicz et al., 1985; Eichwald and Walleczek, 1996). The most evident effects induced by magnetic waves are the mobilization of intracellular Ca and occasionally morphological changes, although cell signals when present are extremely variable (Liburdy et al., 1993; Karabakhtsian et al., 1994; Goodman et al., 1995; Barbier et al., 1996; Loscher and Liburdy, 1998).

Our study is based on the possibility that ELF-EMFs could interfere with dynamic cell conditions such as division, differentiation, and membrane voltage fluctuation as well as changes in intracellular Ca concentrations. During our experiments we used field intensities of the same order of magnitude as those measured in the proximity of household appliances or electric power lines (source http://www.hsph.harvard.edu/organizations/canprevent/emf.html).

All of our experiments, from cell culture to patch-clamp, were performed in the constant presence of a magnetic field. We were not expecting to find that exposure to magnetic fields produces drastic effects on cell physiology. Our aim was to reveal sudden alterations that, in most cases, could well be buffered by alternative cytosolic pathways without triggering degenerative damage to cells.

In the present study we show that ELF-EMFs interfere with the differentiation of NG108-15 neuroblastoma× glioma cells in vitro. The differentiating agent, by acting on the surface charges, modulates the normal "depolarization-repolarization" response to growth factors. The resulting change in cell membrane potential represents the cell's commitment to differentiation (Arcangeli et al., 1987; Olivotto et al., 1996). The mechanism of interaction that we propose exists between electromagnetic fields and chemically induced differentiation is based on two antagonistic cellular events. An ELF-EMF is able to prevent the shift in the surface charge potential and, thereby, hyperpolarization. However, it simultaneously stimulates an increase in intracellular Ca in a dose-dependent manner. By opening Ca-dependent potassium channels, the increase in cytoplasmic divalent ions acts as a rescue agent in cell membrane hyperpolarization, reestablishing the cell's commitment to differentiation. In NG108-15 cells exposed to low intensity ELF-EMFs the two mechanisms appear separate where the magnetic field continues to counteract hyperpolarization but

Received for publication 28 November 2000 and in final form 25 July 2001.

Address reprint requests to Prof. Michele Mazzanti, Dipartimento di Biologia Cellulare e dello Sviluppo Università "La Sapienza," P.le Aldo Moro 5, I-00185, Roma, Italy. Tel.: 39-6-49912683; Fax: 39-2-70263884 / 39-6-49912351; E-mail: michele.mazzanti@uniroma1.it.

0006-3495/01/11/2580/10 $2.00

intracellular Ca is not sufficiently raised. The simultaneous onset of the two mechanisms probably prevents major damage during cell differentiation. Problems with exposure to ELF-EMFs may be linked with pathological situations in the event of a malfunctioning of intracellular Ca control mechanisms.

METHODS

Cell cultures and FACS analysis

Neuroblastoma×glioma culture cells (NG108-15) were grown in Dulbecco's modified Eagle media-high glucose with 10% heat-inactivated fetal calf serum in a 5% CO_2 humidified atmosphere at 37°C (Seidman et al., 1996).

Flow cytometric analyses were performed on cell samples taken after 72 h in the presence of BT2cAMP (96 h of growth). Frequency histograms of propidium iodide (PI)-emitted fluorescence intensity (FL2-height; proportional to the cell DNA content) were obtained from parallel and independent cultures at the indicated field intensities (6 cultures at 0 and 120 μT; 5 cultures at 0 and 360 μT). Signals due to dead cells, cell aggregation, and/or polyploidization contributed to ~10% of the recorded distributions and were discarded before calculating the cell frequencies in G1, S, and G2/M.

Electromagnetic field exposure

A 50-Hz electromagnetic field was continuously provided inside the cell incubator using a Helmoltz device connected to a custom-made variable magnetic field generator. The field was measured at the beginning and end of each experiment. The maximal value of the induced electric field was negligible, ~0.45 mV/m. The cell incubation temperature was 37 ± 0.6°C throughout each experiment and was directly monitored. During patch-clamp whole-cell experiments the magnetic field was delivered by a single copper coil connected to a custom-made variable magnetic field generator placed around the petri dish containing the cells. The ELF-EMF was measured directly before and after each recording using an accurately calibrated custom-made detection device.

Electrophysiology and Ca measurement

Standard whole-cell and perforated-patch voltage- and current-clamp techniques were used. The bath solution (pH 7.32) contained: 133 mM NaCl, 4 mM KCl, 2 mM $MgCl_2$, 2 mM $CaCl_2$, 10 mM HEPES, 5 mM glucose. The electrode solution (pH 7.32) for resting potential monitoring contained: 10 mM NaCl, 120 mM KAsp, 2 mM $MgCl_2$, 4 mM $CaCl_2$, 10 mM HEPES, 10 mM EGTA, 3 mM Mg-ATP, 0.2 mM Na_2-GTP, and amphotericine for experiments in perforated-patch measurements. To record Ca current we used: 72 mM cholineCl, 3 mM KCl, 1 mM $MgCl_2$, 10 mM $CaCl_2$, 10 mM HEPES, 50 mM TEA-Cl, 10 mM 4AP, 24 mM glucose in the bath (pH 7.32) and 20 mM TEA-Cl, 120 mM CsAsp, 2 mM $MgCl_2$, 10 mM HEPES, 10 mM EGTA, 4 mM Mg-ATP, 5 mM CP-Tris, 0.1 mM GTP-Tris, and 20 μ/ml CPK (pH 7.32) to fill the patch-pipette. BT2cAMP (Sigma, Milano, Italy) and other chemicals were added using a fast perfusion system. We used an Axon 200B patch-clamp amplifier (Axon Instruments, Novato, CA) to record membrane voltage and current. Experimental traces were digitized (0.2-ms sampling rate) on a VCR (Panasonic, Milano, Italy). Data were analyzed on a PC computer after filtering at 1000 Hz using pClamp 7 programs (Axon Instruments). For electrophysiological measurements in the presence of an electromagnetic field, the experimental chamber was encircled with an isolated multispiral copper wire to calibrate each field intensity.

Ca was monitored with Indo-1 fluorescence as previously described (Grynkiewicz et al., 1985).

RESULTS

The effects of different field intensities on the growth and differentiation of NG108-15 neuroblastoma×glioma cells are shown in Fig. 1. The cell proliferation rate is altered by the magnetic field only if the cells are chemically induced to differentiate using BT2cAMP. Cell growth inhibition by the differentiating agent was relieved by field strength of between 120 and 240 μT. In contrast, the behavior of cells is not statistically different from that of untreated controls at lower (60 μT) or higher (360 μT) field intensities (Fig. 1 *A*). In particular, after 96 h of growth, cell cultures subjected to a 120- or 240-μT field reached higher densities of 20 to 30% more than the nonstimulated NG108-15 cells, whereas at 360 μT there was no statistically significant variation in cell numbers. Undifferentiated cells showed the same growth rate and final cell density as control cells at every field intensity tested. Thus in our differentiating cell line some of the effects on proliferation of the interaction between the electromagnetic field and differentiation reached their maximum in a specific window of field intensities. To monitor the field effects on the cell cycle of NG108-15 cells we performed flow cytometric analysis of cell DNA content during the differentiation process (Fig. 1 *B*). Three days after the addition of BT2cAMP (96 h of growth) most control cells (0 μT) were found in the G1 phase (71 ± 5%; $n = 6$), whereas the S compartment was nearly empty. Twenty-nine percent ± 0.7% ($n = 6$) of cells showed a double DNA content (2C), as part of the population was still dividing (Fig. 1 *A*, *left*). In comparison, under a 120-μT 50-Hz magnetic field a lower percentage of neuroblastoma cells was reproducibly found in the G1 phase (57 ± 4%; $n = 6$). The population showed a remarkable accumulation of cells in both the S and G2/M phases (13 ± 1% and 30 ± 3%, respectively; $n = 6$) (Fig. 1 *B*). Notably, after 3 days BT2cAMP stimulated the growth of long, branched neurites, whereas these morphological changes were almost completely inhibited by exposure to a 120-μT field (Fig. 1 *C*). Furthermore, in these conditions the average size of the cell bodies in populations subjected to the 120-μT field was larger than in controls, as can be directly appreciated in Fig. 1 *C* and as indicated by a 15 to 30% increase in average forward light scatter values (Fig. 1 *B*). Taken together with the increase in cell numbers, DNA content, and cell morphology, this observation further indicates that proliferation is not inhibited by the differentiating molecule. Significantly, cells exposed to 360 μT showed the same DNA/cell size profile as well as the same morphology as control cells (Fig. 1 *B* (*right*) and *C*), fully confirming that the effects of the magnetic field are not proportional to the intensity but are confined to an intensity window. In conclusion, the differentiating effects elicited by BT2cAMP on NG108-15

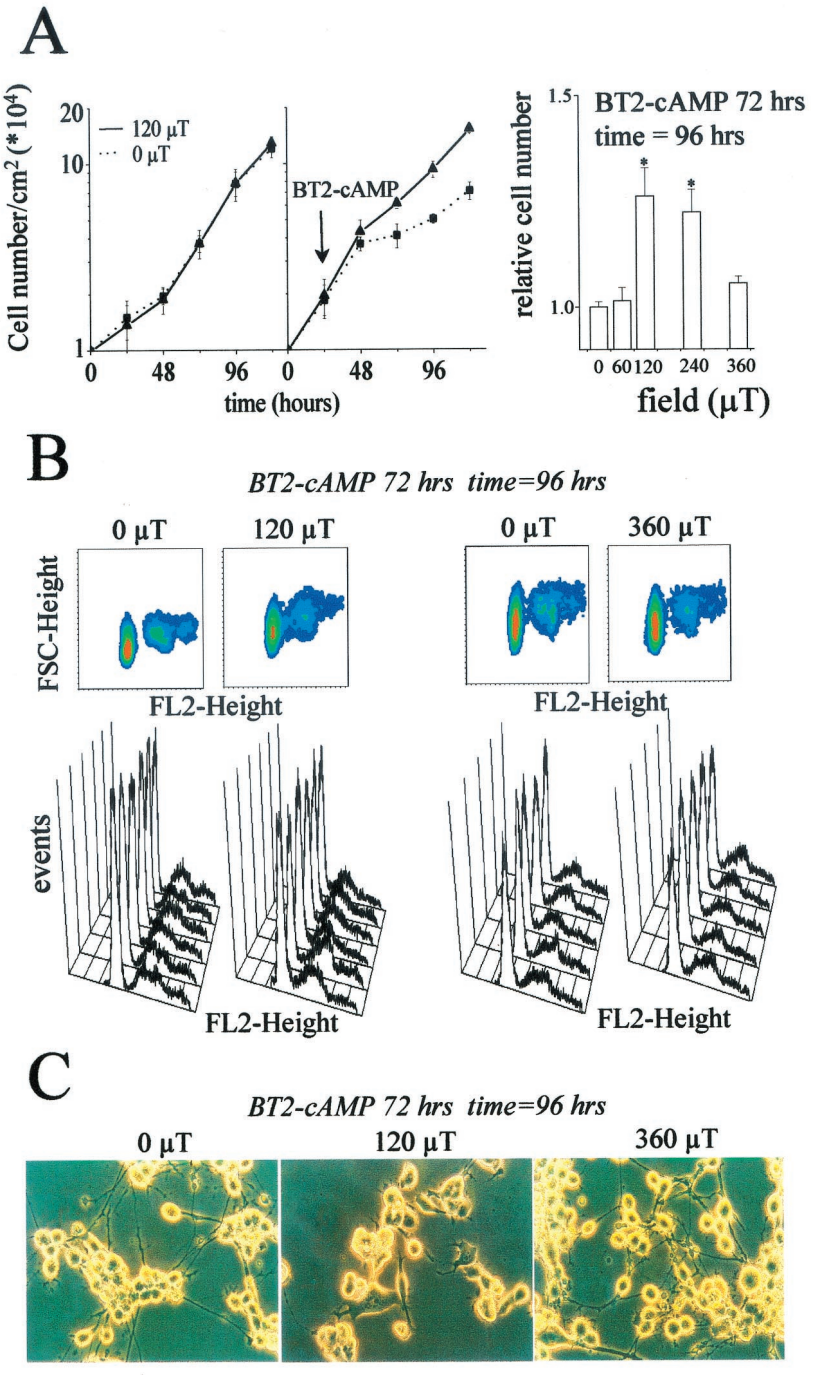

FIGURE 1 Effects of a 50-Hz electromagnetic field on a differentiating neuroblastoma cell line. (*A*) Growth curves of NG108-15 cells in the absence (*dotted line*) and presence (*continuous line*) of a 120-μT field (cell plated at time = 0). Cells were undifferentiated (*left*) or supplied with 1 mM BT2cAMP (*right*) after 24 h (*arrow*). (*Right*) Relative increase in cell numbers after 96 h in BT2cAMP-treated populations. The ratio between the cell numbers reached by cultures at the indicated field intensities and that observed at 0 μT is reported ($n = 25$). (*B*) Distribution of Cell DNA content in differentiating cells exposed to different intensity fields. Flow cytometric analyses were performed on cell samples taken after 72 h in the presence of BT2cAMP (96 h of growth). Frequency histograms of PI-emitted fluorescence intensity (FL2-height; proportional to the cell DNA content) were obtained from parallel and independent cultures at the indicated field intensities (six cultures at 0 and 120 μT; five cultures at 0 and 360 μT). Signals due to dead cells, cell aggregation, and/or polyploidization contributed to ~10% of the recorded distributions and were discarded before calculating the cell frequencies in G1, S, and G2/M (see text). Two representative examples are also shown as density plots between FL2-height and the intensity of forward light scatter (FSC-height; proportional to cell size). A warmer color indicates more events and a cooler color indicates fewer events. (*C*) Phase contrast pictures of differentiating NG108-15 cells exposed to different intensities (0, 120, and 360 μT) of electromagnetic field and supplied with BT2cAMP for 72 h.

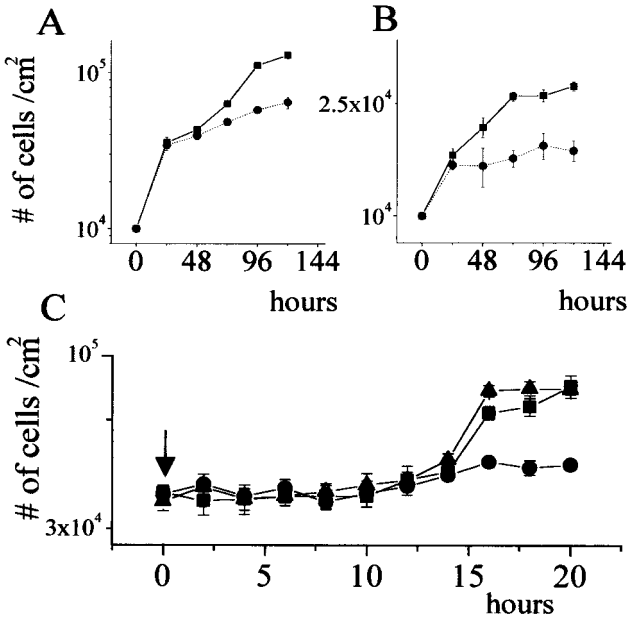

FIGURE 2 (*A*) and (*B*) Growth curve of NG108-15 cells obtained in the presence of 10 μM RA (*A*) or 50 mM DMSO (*B*) with or without the presence of a 120-μT EMF. (*C*) Cell growth in the presence of an EMF using a synchronized cell population. Undifferentiated cells were used to establish the time of the first cell division after release from the synchronized procedure (▲ *solid line*). BT2-cAMP-stimulated cells did not change in number during this interval (● *broken line*). Cells to which the differentiating agent was added and a 50-Hz 120-μT EMF delivered show similar behavior to undifferentiated cells (■ *dotted line*).

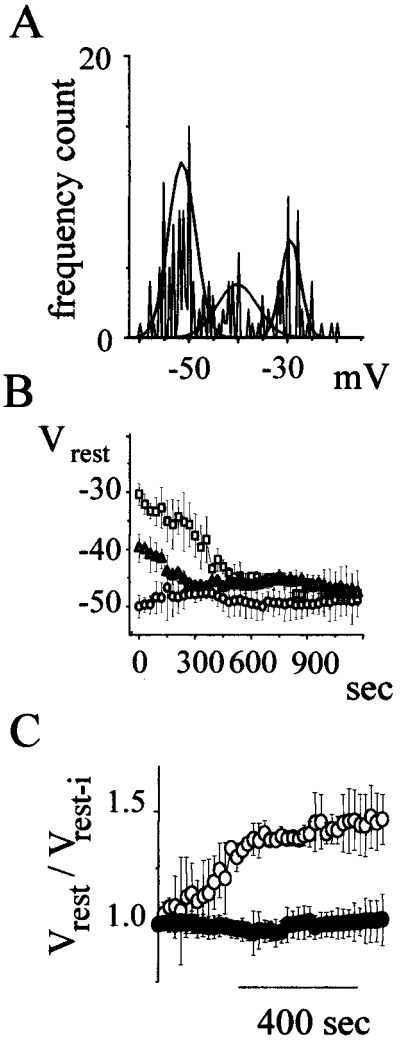

FIGURE 3 Effects of BT2cAMP and a magnetic field on the resting potential of undifferentiated NG108-15 cells. (*A*) Distribution of cell membrane potential values after 24 h in culture (n = 183). Gaussian fitting identifies three main subgroups. (*B*) Membrane potential changes induced by 5 mM BT2cAMP (supplied at time 0) in the three subgroups. Potentials were monitored during whole-cell current-clamp experiments for 20 min (n = 28). The serial resistance value was systematically controlled. (*C*) Averages from experiments in the presence of 5 mM BT2cAMP (○) and during the simultaneous application of 5 mM BT2cAMP and 5 mM Apamine and 1 mM TEA (●) plotted as the ratio between the resting potential at any recorded time (V_{rest}) and the initial resting potential ($V_{rest\text{-}i}$).

cells can be inhibited by an electromagnetic field of between 120 and 240 μT. We obtained similar results using retinoic acid (RA) and dimethyl sulfoxide (DMSO) as inducers of differentiation (Wanke et al., 1979; Olivotto et al., 1996). Fig. 2 shows cell growth curves obtained in the presence of 10 μM RA (Fig. 2 *A*) or 50 mM DMSO (Fig. 2 *B*) with or without the presence of a 120-μT EMF. In both cases the field has a similar effect on cell growth as that already described for BT2-cAMP and reported in Fig. 1 *A*. To strengthen the hypothesis that magnetic fields interfere with the mechanism of differentiation by maintaining cells in a cycling state we repeated the experiment of cell growth in the presence of an EMF using a synchronized cell population. By following the growth rate of synchronized undifferentiated cells we were able to establish the time lapse between release from the synchronized procedure (*arrow* in Fig. 2 *C*) and the first cell division (Fig. 2 *C* (*solid triangle*)). BT2-cAMP-stimulated cells remained almost unchanged during this interval (Fig. 2 *C* (*solid circle*)). Cells in the presence of the differentiating agent and subjected to a 50-Hz 120-μT EMF showed similar behavior to undifferentiated cells (Fig. 2 *C* (*solid square*)).

Most differentiating agents, whether polar or apolar (Wanke et al., 1979), are thought to interfere with growth factor-dependent pathways by acting on surface charges present on the cell membrane (Arcangeli et al., 1987; Olivotto et al., 1996). In undifferentiated NG108-15 cells membrane potential values (V_{rest}) (Ferroni et al., 1996) show a multiple Gaussian distribution that identifies three main subgroups (Fig. 3 *A*), possibly related to different cell-cycle phases (Binggeli and Weinstein, 1985; Dubois and Rouzaire-Dubois, 1993). On average (n = 183) the lowest potential recorded in cells cultured for 24 h was approximately −50 mV. Acute application of the differen-

tiating agent BT2cAMP induced membrane potential hyperpolarization in the cells with a more depolarized V_{rest}. RA and DMSO act in the same way (data not shown), according with the similarity between the results presented in Figs. 1 *A* and 2 *A* and *B*. These cells were driven to a membrane potential of −50 mV within 10 to 15 min (Fig. 3 *B*). Fig. 3 *C* compares the averages of 16 experiments in which eight cells (*solid circles*), in addition to stimulation with BT2cAMP (*open circle*), were exposed to 1 mM TEA and 100 mM Apamin to block Ca-activated K channels (K_{Ca}). The plot shows the rate of V_{rest} over the initial membrane potential value ($V_{rest\text{-}I}$) during 13 min of continuous recording. On average hyperpolarization was fully abolished by the application of K_{Ca} blockers, suggesting a mobilization of intracellular Ca due to the action of the differentiating agent. Voltage-gated Ca channels did not appear to be directly related to this phenomenon, because the application of 1 mM cadmium and 1 mM nickel was not able to prevent BT2-cAMP-induced hyperpolarization (data not shown).

The change in the membrane resting potential due to BT2-cAMP can be correlated with the initial events that occur during commitment to differentiation (Binggeli and Weinstein, 1985; Arcangeli et al., 1993). Because a 120-μT field is able to prevent BT2-cAMP-induced differentiation, we investigated whether an ELF-EMF field might act primarily by affecting V_{rest} hyperpolarization. Fig. 4 *A* shows how, after BT2cAMP application (*open square*), cell hyperpolarization is completely abolished by the constant presence of an ELF-EMF at 120-μT intensity (Fig. 4 *A* (*filled square*)). In Fig. 4 *B* the average results obtained in 14 cells (7 control (*solid circles*) vs. 7 ELF-EMF-treated cells (*open circles*)) are shown. In all cases the 120-μT field suppressed the hyperpolarizing effects of BT2cAMP.

The question arises about the possibility that the prevention of BT2-cAMP hyperpolarization by an EMF is mediated by an opposite action on the surface charges. We therefore performed experiments to test the influence of adding to the external milieu two ions that are known to act, inter alia, on the surface charges of the cell membrane (Kajimoto and Kirpekar, 1972; Zipes and Mendez, 1973; Dorrscheidt-Kafer, 1981; Sanguinetti and Jurkiewicz, 1990). Fig. 5 shows the changes induced by 10 μM La^{3+} (Fig. 5 *A*) and Mn^{2+} (Fig. 5 *B*) in the membrane resting potential of NG108-15 cells and the consequent action of 120- and 240-μT 50-Hz EMFs. Both La^{3+} and Mn^{2+} -induced depolarization was enhanced by increasing the strength of the field. However, the present results were inconsistent and repeatable only in 50% of the experiments (7 of 14 trials). In the others, the action of the di- and trivalent ions either produced no effect ($n = 4$) or induced slight hyperpolarization ($n = 2$) or 70-mV depolarization ($n = 1$). For our experiments we then used the 50% of cells in which BT2-cAMP and La^{3+} independently and reproducibly provoked a change in V_{rest}. In the sequence of Fig. 5 *C* we show the hyperpolarizing effect of BT2-cAMP, the

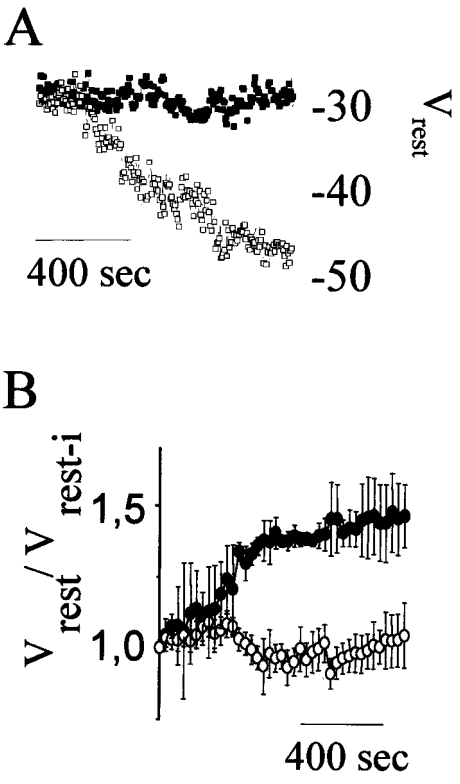

FIGURE 4 Effects of a 120-μT ELF-EMF on BT2-cAMP-induced hyperpolarization. (*A*) Membrane voltage recording performed on a single cell initially showing a −30-mV resting potential in the presence (■) or in the absence (□) of a 120-μT electromagnetic field. (*B*) Average results obtained with more cells exposed (○) or not (●) to the field as the ratio between the resting potential at any recorded time (V_{rest}) and the initial resting potential ($V_{rest\text{-}i}$). Recording was made by whole-cell ($n = 3$) or perforated-patch experiments ($n = 2$).

null combined action of BT2-cAMP, and a 120-μT ELF-EMF, the depolarizing effect of 10 μM La^{3+}, followed by the enhanced action of an EMF. The simultaneous presence of the differentiating agent and the trivalent cation did not change the cell membrane potential. In the latter conditions the application of a 120-μT magnetic field caused slight depolarization. The time interval between different stimulation procedures was 10 min in each experiment presented in Fig. 5.

In contrast to a 120-μT ELF-EMF, the application of a 360-μT field did not alter the hyperpolarization induced by the differentiating molecule. This result is in agreement with the data obtained on growth curve experiments (Fig. 1). In the example of Fig. 6 *A* we show that the hyperpolarization induced by the contemporary presence of BT2-cAMP and a 360-μT field (*open squares*) can be eliminated by 1-mM TEA and 100-mM Apamin (*filled squares*), confirming the involvement of K_{Ca} in the modification of the membrane potential. Significantly, a 360-μT ELF-EMF by itself (Fig. 6 *B* (*open circles*)) was able to reproduce the hyperpolarization due to the differentiating agent (*solid circle*). How-

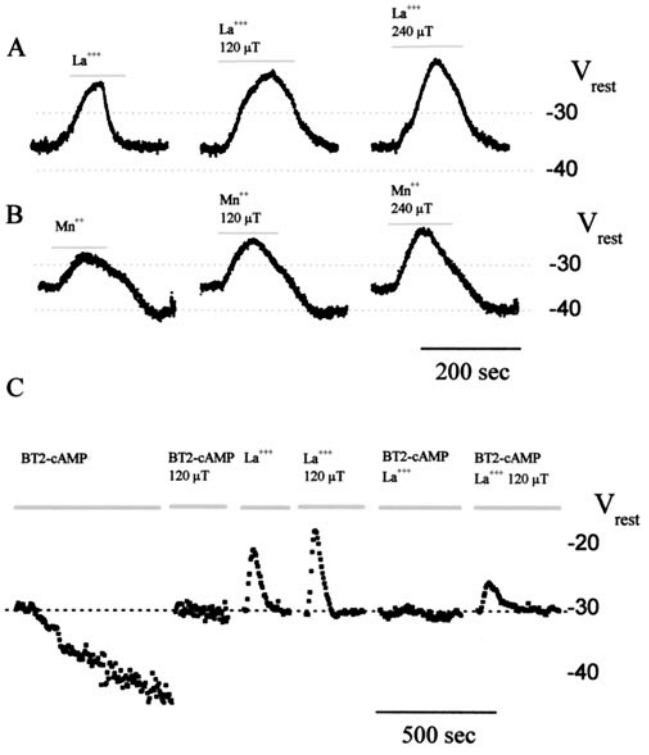

FIGURE 5 Effects of La^{3+} and Mn^{2+} on cell membrane potential. The figure depicts the changes induced by 10 μM La^{3+} (Fig. 5 *A*) and Mn^{2+} (Fig. 5 *B*) in the membrane resting potential of NG108-15 cells and the increment in depolarization caused by 120- and 240-μT 50-Hz EMFs. Figure 5 *C* shows a sequence of: hyperpolarizing effect of BT2-cAMP, null action of BT2-cAMP when a 120-μT ELF-EMF is simultaneously present, depolarizing effect of 10 μM La^{3+}, enhanced action of EMF, no changes in the membrane potential during the simultaneous presence of BT2-cAMP and La^{3+} and slight depolarization caused by a 120-μT ELF-EMF applied in the latter conditions.

ever, although the final target is the same, namely the K_{ca} current, the mechanism of intracellular Ca mobilization promoted by a 360-μT 50-Hz field appears to be different. In particular, 10-mM Nifedipine (Fig. 6 *C* (*solid squares*)) prevents the hyperpolarization due to a 360-μT ELF-EMF (Fig. 6 *C* (*open circles*)), contrary to what we observed in the case of BT2-cAMP-induced hyperpolarization, as previously stated. Nickel (1 mM) and cadmium (1 mM), or total removal of extracellular Ca also impaired hyperpolarization at a field intensity of 360 μT (data not shown). In Fig. 6 *D* we report experimental averages in the different conditions (BT2-cAMP stimulation, $n = 7$, *open circles*; 360-μT ELF-EMF, $n = 8$, *open squares*; 360-μT ELF-EMF, Nifedipine block, $n = 12$, *solid squares*). To provide further support for the hypothesis of a Ca ion-mediated effect during electromagnetic field exposure, we constructed growth curves of NG108-15 cells in the presence of an EMF and low external Ca (Fig. 7). In this case the difference in cell growth observed in the experiments of Fig. 1 *B* is present not only at intensities of 120- (Fig. 7 *A*) and 240-μT (Fig. 7 *B*) ELF-EMFs, but also at 360 μT (Fig. 7 *C*). Fig. 7 *D* depicts the comparison between cells cultured in the constant presence of a magnetic field with 1.8 (*gray bars*) and 0.1 mM (*black bars*) external Ca ($n = 6$).

The results reported in Figs. 6 and 7 together with previous studies (Goodman et al., 1995) argue in favor of an interaction between magnetic fields and the mechanisms that regulate intracellular Ca mobilization. Measurement of the intracellular Ca signal by Indo-1 fluorescence during ELF-EMF irradiation (Grynkiewicz et al., 1985) could furnish direct evidence of the dynamics of the divalent ions under the influence of magnetic fields. Intracellular Ca concentration rose modestly if a 120-μT magnetic field was applied (Fig. 8 *A*, $n = 18$). The increase was much greater under a 360-μT field ($n = 4$). When we changed the intensity of the field applied to a single cell (Fig. 8 *B*) the increase in intracellular Ca was 3 times greater at 360 μT than at 120 μT.

We investigated the possibility that BT2cAMP and a 120-μT 50-Hz magnetic field could interact antagonistically during the differentiating process by affecting the membrane surface charges. To this end we monitored the activation properties of the low-threshold Ca current (Becchetti et al., 1992) in undifferentiated NG108-15 cells challenged by BT2cAMP and/or an electromagnetic field. In the example in Fig. 9 *A*, currents were recorded with or without a voltage step (from -50 to $+10$ mV) during continuous cell exposure to a 120-μT field. Ca current was obtained by subtracting the trace in the absence of the voltage challenge (bottom). This procedure was used to construct the activation curve of a low-threshold Ca current in the presence of a 120-μT field (Fig. 9 *B*). The comparison with control cells ($n = 7$) and cells treated with BT2cAMP ($n = 5$) showed that the magnetic field and the differentiating agent had opposing effects, shifting the activation curves respectively to more positive or negative potentials (*top*). This was confirmed in cells simultaneously exposed to BT2cAMP and a 120-μT field in which the shifts were not observed ($n = 4$) (*bottom*). The effect of an ELF-EMF on surface charges is proportional to the field intensity. Figure 9 *C* shows that the shift of an L-type Ca current activation curve toward a more negative potential averages ± 4 at 120, ± 5.6 at 240, and ± 7.4 at 360 μT.

DISCUSSION

Despite growing concern about electromagnetic radiation, the physical mechanisms of interactions between 50/60-Hz fields and biological structures remain obscure. So far biophysical models can provide only indications of the mechanisms underlying the reported field effects (e.g., local field effect at the cell membrane, including interference with the surface charges of the plasmalemma or with ligand-receptor binding) (Walleczek, 1992). Most investigations have been carried out on immune system cells because epidemiologi-

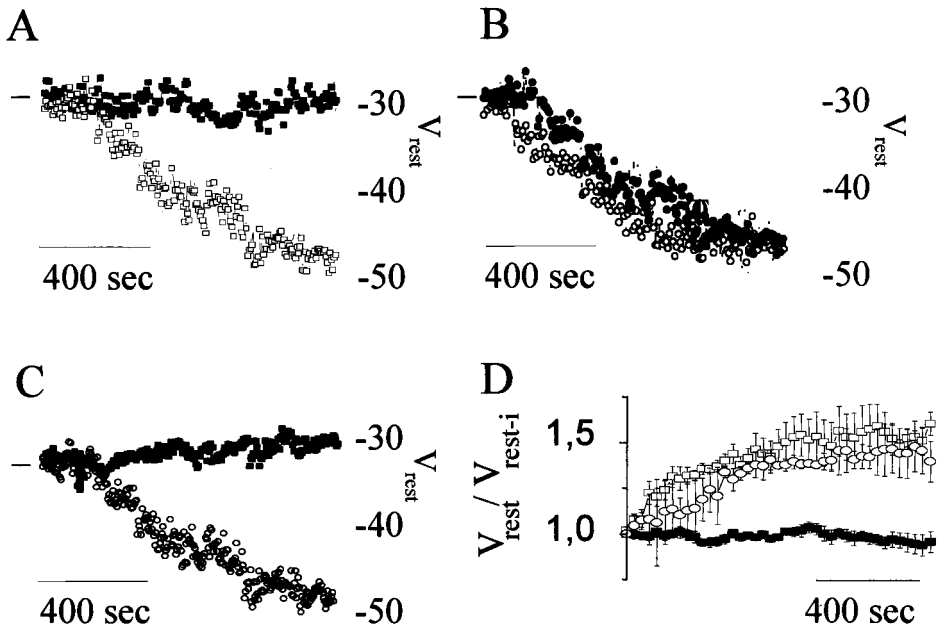

FIGURE 6 Effect of a 360-μT ELF-EMF on undifferentiated NG108-15 cells. (*A*) Single-cell measurements in the simultaneous presence of 5 mM BT2-cAMP and a 360-μT magnetic field with (■) or without (□) the addition of 5 mM apamine and 1 mM TEA in the bath solution. (*B*) Comparison between the cell membrane hyperpolarization induced by 5 mM BT2-cAMP (●) and by a 360-μT ELF-EMF (○). (*C*) Ten micromolars nifedipine (■) completely prevents the hyperpolarization produced by exposure of the cell to a 360-μT ELF-EMF (○). (*D*) Relative membrane potential changes. 0 μT (○, $n = 7$), 360 μT (□, $n = 8$), or 360 μT field + apamine + TEA (■, $n = 12$).

cal studies have shown a correlation between exposure to ELF-EMFs and childhood leukemia (Lacy-Hulbert et al., 1995). These studies indicated the Ca signal as a plausible candidate for the mediation of ELF-EMF effects on cell processes. However, the action of magnetic fields on Ca regulation at the molecular level is still poorly understood. Many reports have demonstrated that ELF-EMFs do not affect the extent of Ca release from intracellular stores but increase Ca influx through the plasma membrane (Karabakhtsian et al., 1994; Liburdy, 1992; Fanelli et al., 1999).

In this paper we have tried to accumulate data to support the hypothesis that extremely low electromagnetic fields act primarily on the surface charges of the cell membrane. Our results show that ELF-EMFs: 1) disturb the action of several differentiating agents (Fig. 2); 2) enhance the interaction of La^{3+} and Mn^{2+} with the cell membrane (Fig. 5); 3) modify intracellular Ca and Ca-related mechanisms in a dose-dependent way (Fig. 9). A magnetic field of 50 Hz, which approximates the magnitudes measured in the proximity of household appliances or electric power lines (source http://www.hsph.harvard.edu/organizations/canprevent/emf.html), is probably not sufficient to trigger primary cell functions directly. We think it more probable that, by acting on cell membrane surface charges the magnetic field acts as a destabilizing agent of complex protein-to-protein interactions that occur, for example, during the cell differentiation process, although at present we have no reason to believe that this is the only mechanism through which ELF-EMFs

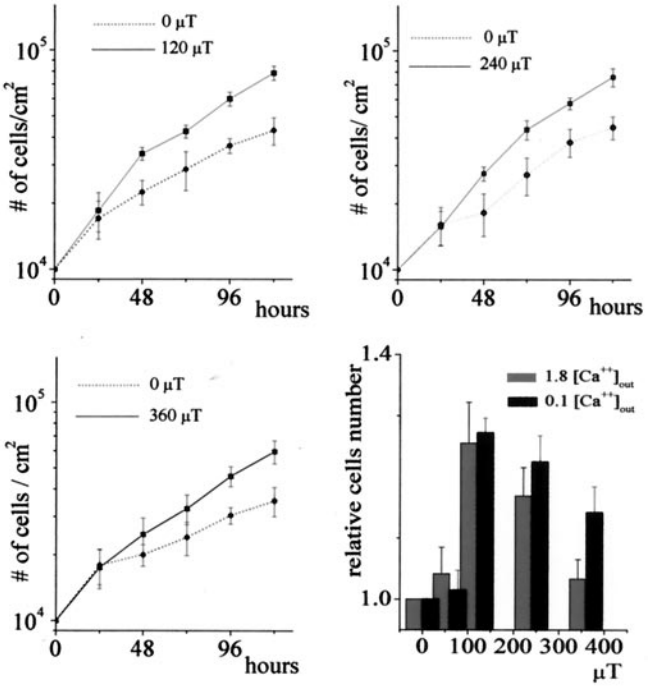

FIGURE 7 Growth curves of NG108-15 cells in the presence of an EMF and low external Ca. The difference in cell growth between cells exposed to a magnetic field and controls is always present: at 120-μT (*A*), at 240-μT (*B*), and at 360-μT (*C*). (*D*) Comparison between cells cultured in the constant presence of a magnetic field with 1.8 (*gray bars*) and 0.1 (*black bars*) mM external Ca ($n = 6$).

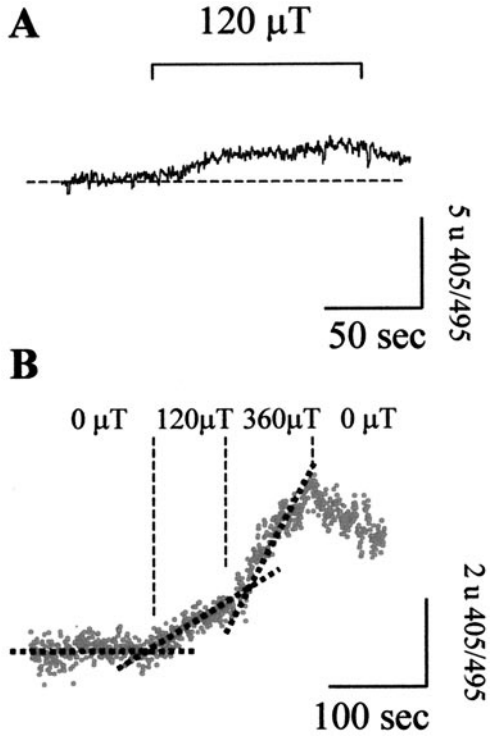

FIGURE 8 Effect of an electromagnetic field on intracellular Ca. (*A*) Intracellular Ca in a single cell subjected to a 120-μT field intensity. (*B*) Intracellular Ca increased in a single cell sequentially exposed to 0-, 120-, 360-, and again 0-μT intensity fields; data were fitted by linear regression for each interval at the specific field intensity.

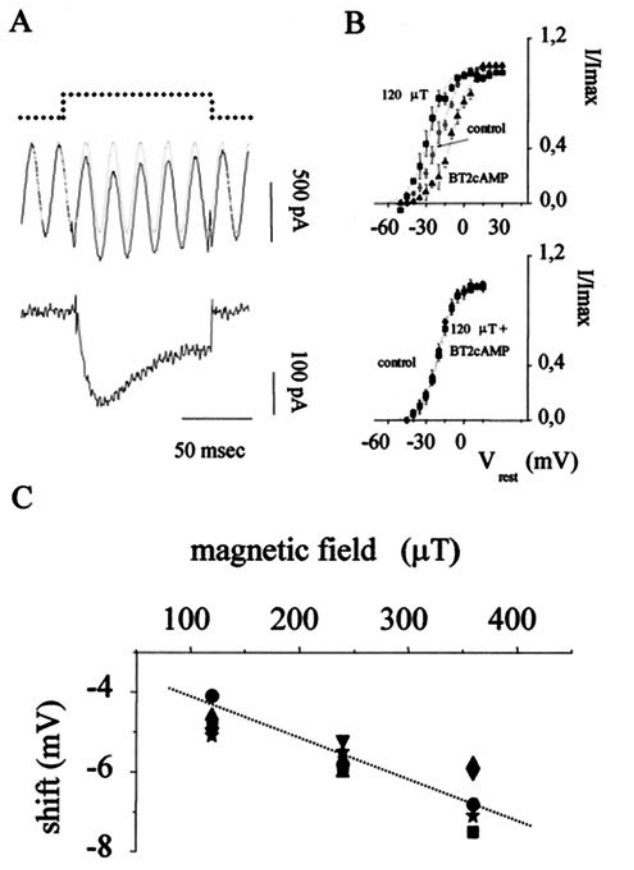

FIGURE 9 Low-threshold Ca current in cells challenged by an electromagnetic field and BT2cAMP. (*A*) Example of whole-cell Ca current recordings during continuous exposure of cells to a 120-μT field (*bottom*). Current traces were obtained by digital subtraction after (*top, thin line*) and before (*top, thick line*) the application of a voltage step (from holding potential of -50 to $+$ 10 mV). (*B*) The top panel depicts activation curves of low-threshold Ca current obtained in control cells ($n = 7$) (●) after perfusion with 5 mM BT2cAMP ($n = 5$) (▲) and in the presence of a 120-μT field ($n = 5$) (■) (in this case using the method described in *A*). The lower panel shows low-threshold Ca current activation curves in control conditions (●) and during the simultaneous presence of a 120-μT electromagnetic field and 5 mM BT2cAMP ($n = 4$) (■). (*C*) Results of five experiments in which the activation-curve negative shift was calculated and plotted as a function of the increasing electromagnetic field delivered.

may interact with biological material. A direct action on single proteins and/or the activation of ion transporters could reasonably take place. Alternatively, magnetic fields could have an as yet unidentified effect on water molecules. Regardless of the mechanisms involved, the final conclusion of our work is that a repeatable and consistent interaction between ELF-EMFs and some biological functions does exist.

The results we obtained concerning the opposite effects on Ca current activation curves promoted by an ELF-EMF and by the differentiating agent (Fig. 9), together with the data obtained using La^{3+} and Mn^{2+} (Fig. 5), could be a sufficient indication that the field interacts with the surface charges on the plasma membrane. Our conclusion is supported by the study of Arcangeli et al. (1993) showing the modulation of surface charges by different classes of differentiating agents. To demonstrate the hypothesis of an interaction between surface charges and ELF-EMFs, we directed our attention to the effects that changes in the surface potential may have on Ca-dependent processes. We therefore attempted to understand which Ca permeation pathway was directly involved. Specifically, we considered the role of voltage-gated Ca channels in the Ca protection of cell differentiation during exposure to an ELF-EMF. The model we suggest to explain the effect of a low magnetic field on induced differentiation of the NG108-15 cell line is the following: 1) growth factors contained in fetal calf serum are able to promote depolarization-repolarization of membrane potentials fundamental for progression of the cell-cycle (Arcangeli et al., 1987); 2) a coupling between growth factor receptors and various effector proteins allow regulation of the Ca influx through an undetermined molecular pathway. As a consequence of Ca influx, the K_{Ca} opens, leading to cell hyperpolarization. When cytoplasmic buffers lower intracellular Ca, the K_{Ca} closes and the cell again depolarizes (Conley, 96); 3) differentiating agents slow down the depolarization-repolarization process of membrane potentials adsorbing at the charged surface. The

inducer first affects the Ca influx, which then activates the K_{Ca} (Arcangeli et al., 1987; Conley, 96).

Membrane potential measurements, obtained in the constant presence of complete culture medium, showed hyperpolarization during acute application of 5 mM BT2-cAMP (Fig. 3 *B*). The effect was detectable in a cell subpopulation with membrane resting potential more depolarized than −50 mV. In particular the cell population with a membrane resting potential of −30 mV is likely to be in a specific cell cycle phase and can be identified using the "inducible" cells reported in the paper by Arcangeli et al. (1987). It has been previously suggested that chronic hyperpolarization of the membrane potential might actually inhibit progression through cell cycle (Binggeli and Weinstein, 1985). In our experiments we show that the acute application of Bt-cAMP results in a sustained hyperpolarization, as large as cells are depolarized. In the presence of Bt2-cAMP the resting membrane potential is held at value close to −50 mV, possibly impairing all the cell cycle process that would respond only to a change in membrane potential (Binggeli and Weinstein, 1985). Base on this view, the ultimate effects of Bt2-cAMP on cell replication would therefore take at last a period of time close to the Td (duplication time) to be manifested.

This idea is supported by our experiment on synchronized cells (Fig. 2). Growth curves split between EMF-stimulated cells and controls occurred in the time lapse of the first cell division. Apamine/TEA, prevented the hyperpolarization (Fig. 3 *C*), in agreement with the role of the K_{Ca} in a depolarization-repolarization process modulated by the differentiating agent (Conley, 96). Experiments reported in our study show that neither nickel/cadmium or Nifedipine prevented the hyperpolarization induced by BT2-cAMP. In Fig. 9 we show that BT2-cAMP shifts the activation curve of low-threshold Ca current to more positive potentials (+10 mV) in agreement with its effect on surface charges (Arcangeli et al., 1993). This result indicates that at −30 mV, the mean resting potential of a BT2-cAMP-responsive cell population, the current carried by the voltage-gated Ca channel, is reduced in the presence of BT2-cAMP, and voltage-dependent Ca currents can therefore not account for activation of the K_{Ca}.

This last consideration suggests that in our system BT2-cAMP interferes with the surface potential and indirectly increases K_{Ca} activity, modulating the Ca influx not through voltage-gated Ca channels. It was previously stated that extracellular Ca mediated the depolarization-repolarization process rather than the release of Ca from the stores (Arcangeli et al., 1987). In this case, the shift in the activation curve of L-type Ca channels promoted by BT2-cAMP is only an indirect effect of changes in the surface charges with no relevance for the mechanisms underlying BT2-cAMP-induced hyperpolarization.

ELF-EMF (120 μT) completely prevents BT2-cAMP-induced hyperpolarization (Fig. 4). The magnetic field appears to cause a shift in the surface potential in the opposite direction to that caused by BT2-cAMP. In the experiment in Fig. 5 *C* we produce direct evidence supporting this behavior. The contemporary presence of La^{3+} and BT2-cAMP completely abolish the change in membrane potential. Furthermore, the effect of ELF-EMF, applied in these experimental conditions, promoted a slight depolarization (Fig. 5 *C*), increasing the effect of La^{3+}. Further experimental evidence, probably of greater physiological significance, was obtained using L-type Ca currents as voltage sensors of surface potential. Because the shift in the activation curves promoted by BT2-cAMP is not directly related to hyperpolarization, the primary effect of a 120-μT ELF-EMF may counteract the adsorption of BT2-cAMP to the surface charges. A 360-μT ELF-EMF, in contrast, was able to hyperpolarize the cell both in the presence and in the absence of the differentiating agent (Fig. 6 *B*). Hyperpolarization was prevented by Apamine/TEA (Fig. 6 *A*) as well as by Nifedipine (Fig. 6 *C*) or by nickel/cadmium (data not shown). This is the major factor indicating that, in the presence of a 360-μT ELF-EMF, the magnitude of the shift in the surface potential is able to increase the amount of the Ca current through L-type channels. The increment is likely to be sufficient to activate K_{Ca}, independently of the mechanisms that couple growth factor receptors and Ca influx. We were able to separate the Ca influx dependent on growth factor stimulation and the Ca permeating through L-type channels because in undifferentiated NG108-15 cells the density voltage-dependent Ca current is very low (Lukyanetz, 1998). Although 120-μT ELF-EMF shifts the activation of the Ca current, the current density is too low to activate K_{Ca} independently of BT2-cAMP. At 360 μT, this shift is greater and an additional mechanism is therefore turned on, antagonizing the primary effect on differentiation due to ELF-EMF interaction with surface charges.

In conclusion, the L-type voltage gated Ca channel primarily mediates the protection by Ca of differentiating neuroblastoma cells from EMF insults. Our initial hypothesis was that the magnetic field could interfere with cell division, differentiation, and membrane voltage fluctuations, possibly by altering intracellular Ca concentration. In our study we demonstrate that a 50/60-Hz magnetic field interacts with cell differentiation through two opposing mechanisms. ELF-EMF is able to prevent the shift in surface charges potential promoted by differentiating agents. Simultaneously, it stimulates the increase in intracellular Ca in a dose-dependent manner. The increase in cytoplasmic divalent ions, by opening the K_{Ca}, acts as a rescue agent reestablishing cell's commitment to differentiation. The peculiarity of NG108-15 cells (Lukyanetz, 1998) offered the possibility to dissect these two opposing mechanisms. The simultaneous onset of both mechanisms prevents alterations in differentiation. We propose that cells are normally protected against electromagnetic insult. The scenario just described might be very different in cells with an efficient Ca permeability system (Brown and Higashida, 1988a, 1988b).

In these cases, the onset of Ca-dependent hyperpolarization induced by the magnetic field would be expected to be more efficient and the above mechanisms difficult to dissociate. The inhibition of differentiation exerted at particular field intensities could be compensated by the ability to mobilize Ca ions. On this basis, Ca signaling may be seen as an agent protecting against damages produced by exposure to electromagnetic fields. In the presence of even silent alterations in mechanisms acting on intracellular Ca or K_{Ca} channels, chronic exposure to magnetic fields might induce pathological conditions. These considerations may help to explain the contrasting results obtained in epidemiological studies in which no significant correlation between electromagnetic exposure and pathological insurgency could be found (Reipert et al., 1997; Lacy-Hulbert et al., 1998; Hatch et al., 1998; Day, 1999).

REFERENCES

Arcangeli, A., M. Carla, M. R. Del Bene, A. Becchetti, E. Wanke, and M. Olivotto. 1993. Polar/apolar compounds induce leukemia cell differentiation by modulating cell-surface potential. *Proc. Natl. Acad. Sci. U.S.A.* 90:5858–5862.

Arcangeli, A., L. Ricupero, and M. Olivotto. 1987. Commitment to differentiation of murine erythroleukemia cells involves a modulated plasma membrane depolarization through Ca2+-activated K+ channels. *J. Cell. Physiol.* 132:387–400.

Barbier, E., B. Dufy, and B. Veyret. 1996. Stimulation of Ca2+ influx in rat pituitary cells under exposure to a 50 Hz magnetic field. *Bioelectromagnetics.* 17:303–311.

Becchetti, A., A. Arcangeli, M. R. Del Bene, M. Olivotto, and E. Wanke. 1992. Intra and extracellular surface charges near Ca2+ channels in neurons and neuroblastoma cells. *Biophys. J.* 63:954–965.

Binggeli, R. and R. C. Weinstein. 1985. Deficits in elevating membrane potential of rat fibrosarcoma cells after cell contact. *Cancer Res.* 45: 235–241.

Brown, D. A. and H. Higashida. 1988a. Membrane current responses of NG108-15 mouse neuroblastoma × rat glioma hybrid cells to bradykinin. *J. Physiol.* 397:167–184.

Brown, D. A. and H. Higashida. 1988b. Voltage- and calcium-activated potassium currents in mouse neuroblastoma × rat glioma hybrid cells. *J. Physiol.* 397:149–165.

Conley, E. C. 96. Intracellular calcium-activated K+ channels (KCa). *In* The Ion Channel Facts Book: Intracellular Ligand-Gated Channels. E.C. Conley, editor. Academy Press, New York. 621–623.

Day, N. 1999. Exposure to power-frequency magnetic fields and the risk of childhood cancer. *Lancet.* 354:1925–1931.

Dorrscheidt-Kafer, M. 1981. Comparison of the action of La3+ and Ca2+ on contraction threshold and other membrane parameters of frog skeletal muscle. *J. Membr. Biol.* 62:95–103.

Dubois, J. M. and B. Rouzaire-Dubois. 1993. Role of potassium channels in mitogenesis. *Prog. Biophys. Mol. Biol.* 59:1–21.

Eichwald, C. and J. Walleczek. 1996. Model for magnetic field effects on radical pair recombination in enzyme kinetics. *Biophys. J.* 71:623–631.

Fanelli, C., S. Coppola, R. Barone, C. Colussi, G. Gualandi, P. Volpe, and L. Ghibelli. 1999. Magnetic fields increase cell survival by inhibiting apoptosis via modulation of Ca2+ influx. *FASEB J.* 13:95–102.

Ferroni, A., A. Galli, and M. Mazzanti. 1996. Functional role of low-voltage-activated dihydropyridine-sensitive Ca channels during the action potential in adult rat sensory neurones. *Pflugers Arch. Eur. J. Physiol.* 431:954–963.

Feychting, M., A. Ahlbom, and D. Savitz. 1998. Electromagnetic fields and childhood leukemia. *Epidemiology.* 9:225–226.

Goodman, E. M., B. Greenebaum, and M. T. Marron. 1995. Effects of electromagnetic fields on molecules and cells. *Intl. Rev. Cytol.* 158: 279–338.

Grynkiewicz, G., M. Poenie, and R. Y. Tsien. 1985. A new generation of Ca2+ indicators with greatly improved fluorescence properties. *J. Biol. Chem.* 260:3440–3450.

Hatch, E. E., M. S. Linet, R. A. Kleinerman, R. E. Tarone, R. K. Severson, C. T. Hartsock, C. Haines, W. T. Kaune, D. Friedman, L. L. Robison, and S. Wacholder. 1998. Association between childhood acute lymphoblastic leukemia and use of electrical appliances during pregnancy and childhood. *Epidemiology.* 9:234–245.

Hojevik, P., J. Sandblom, S. Galt, and Y. Hamnerius. 1995. Ca2+ ion transport through patch-clamped cells exposed to magnetic fields. *Bioelectromagnetics.* 16:33–40.

Kajimoto, N. and S. M. Kirpekar. 1972. Effect of manganese and lanthanum on spontaneous release of acetylcholine at frog motor nerve terminals. *Nat. New Biol.* 235:29–30.

Karabakhtsian, R., N. Broude, N. Shalts, S. Kochlatyi, R. Goodman, and A. S. Henderson. 1994. Calcium is necessary in the cell response to EM fields. *FEBS Lett.* 349:1–6.

Lacy-Hulbert, A., J. C. Metcalfe, and R. Hesketh. 1998. Biological responses to electromagnetic fields. *FASEB J.* 12:395–420.

Lacy-Hulbert, A., R. C. Wilkins, T. R. Hesketh, and J. C. Metcalfe. 1995. Cancer risk and electromagnetic fields. *Nature.* 375:23.

Liburdy, R. P. 1992. Calcium signaling in lymphocytes and ELF fields: evidence for an electric field metric and a site of interaction involving the calcium ion channel. *FEBS Lett.* 301:53–59.

Liburdy, R. P., D. E. Callahan, J. Harland, E. Dunham, T. R. Sloma, and P. Yaswen. 1993. Experimental evidence for 60 Hz magnetic fields operating through the signal transduction cascade: effects on calcium influx and c-MYC mRNA induction. *FEBS Lett.* 334:301–308.

Loscher, W. and R. P. Liburdy. 1998. Animal and cellular studies on carcinogenic effects of low frequency (50/60-Hz) magnetic fields. *Mutat. Res.* 410:185–220.

Lukyanetz, E. A. 1998. Diversity and properties of calcium channel types in NG108–15 hybrid cells. *Neuroscience.* 87:265–274.

Olivotto, M., A. Arcangeli, M. Carla, and E. Wanke. 1996. Electric fields at the plasma membrane level: a neglected element in the mechanisms of cell signalling. *Bioessays.* 18:495–504.

Reipert, B. M., D. Allan, S. Reipert, and T. M. Dexter. 1997. Apoptosis in haemopoietic progenitor cells exposed to extremely low-frequency magnetic fields. *Life Sci.* 61:1571–1582.

Sanguinetti, M. C. and N. K. Jurkiewicz. 1990. Lanthanum blocks a specific component of IK and screens membrane surface change in cardiac cells. *Am. J. Physiol.* 256:881–889.

Seidman, K. J. N., J. H. Barsuk, R. F. Johnson, and J. A. Weyhenmeyer. 1996. Differentiation of NG108–15 neuroblastoma cells by serum starvation or dimethyl sulfoxide results in marked differences in angiotensin II receptor subtype expression. *J. Neurochem.* 66:1011–1018.

Thomson, R. A., S. M. Michaelson, and Q. A. Nguyen. 1988. Influence of 60-Hertz magnetic fields on leukemia. *Bioelectromagnetics.* 9:149–158.

Walleczek, J. 1992. Electromagnetic field effects on cells of the immune system: the role of calcium signaling. *FASEB J.* 6:3177–3185.

Wanke, E., E. Carbone, and P. L. Testa. 1979. K^+ conductance modified by a titratable group accessible to protons from the intracellular side of the squid axon membrane. *Biophys. J.* 26:319–324.

Zipes, D. P. and C. Mendez. 1973. Action of manganese ions and tetrodotoxin on atrioventricular nodal transmembrane potentials in isolated rabbit hearts. *Circul. Res.* 324:447–454.